LNF-97/023

Residual Stress in Polycrystalline Diamond/Ti–6A1–4V Systems

P. Scardi, M. Leoni, G. Cappuccio, V. Sessa, M.L. Terranova

Diamond and Related Materials Vol. 6, 807–811, (1997)

Reprinted from

DIAMOND AND RELATED MATERIALS

Diamond and Related Materials 6 (1997) 807–811

Residual stress in polycrystalline diamond/Ti–6Al–4V systems

Paolo Scardi [a], Matteo Leoni [a], Giorgio Cappuccio [b,*], Vito Sessa [c], Maria Letizia Terranova [c]

[a] *Dipartimento di Ingegneria dei Materiali, Università di Trento, 38050 Mesiano, (TN), Italy*

[b] *Istituto di Strutturistica Chimica, CNR, Monterotondo Staz., and Laboratorio Dafne Luce, INFN – LNF, P.O.B. 13, 00044 Frascati, (RM), Italy*

[c] *Dip. di Scienze e Tecnologie Chimiche, Università di Tor Vergata, Via della Ricerca Scientifica, 00133 Roma, Italy*

ELSEVIER

ELSEVIER

Diamond and Related Materials 6 (1997) 807–811

DIAMOND AND RELATED MATERIALS

Residual stress in polycrystalline diamond/Ti–6Al–4V systems

Paolo Scardi [a], Matteo Leoni [a], Giorgio Cappuccio [b,*], Vito Sessa [c], Maria Letizia Terranova [c]

[a] *Dipartimento di Ingegneria dei Materiali, Università di Trento, 38050 Mesiano, (TN), Italy*

[b] *Istituto di Strutturistica Chimica, CNR, Monterotondo Staz., and Laboratorio Dafne Luce, INFN – LNF, P.O.B. 13, 00044 Frascati, (RM), Italy*

[c] *Dip. di Scienze e Tecnologie Chimiche, Università di Tor Vergata, Via della Ricerca Scientifica, 00133 Roma, Italy*

Abstract

Polycrystalline diamond coatings were deposited on Ti–6Al–4V alloy by HF-CVD, at fixed temperature (650°C) for different deposition times. During the process, thick titanium carbide layers were formed at the metal/diamond interface. X-ray diffraction (XRD) methods were used to assess coating quality, phase composition, texture, and residual macrostress of the diamond/TiC/Ti system. For a better evaluation of the residual stress present in each phase, three independent measurements were performed with synchrotron radiation (SR-XRD). The measured residual strain could be interpreted in terms of a simple axially uniform residual stress model: $\sigma_{11}=\sigma_{22}$, $\sigma_{33}=0$, $\sigma_{ij}=0$ $(i\neq j)$. Irrespective of film thickness, the residual stress was very intense, compressive both in the diamond layer (approx. −6.5 GPa) and in TiC (approx. −1.4 GPa), and tensile in Ti–6Al–4V (approx. 70 MPa). The high residual strain in the diamond layer affected the results of texture measurements using the traditional pole figure method; more reliable results were obtained by measuring the integrated intensity, rather than peak maximum intensity, as a function of tilting angles. © 1997 Elsevier Science S.A.

Keywords: Diamond films; CVD; Ti–6Al–4V; Interface/interfacial; Residual stress; Strain; Texture; Synchrotron radiation; X-ray diffraction

1. Introduction

Residual stress and texture determination is one of the major issues in the development of new coatings and thin films; this is particularly true for polycrystalline diamond layers deposited on metals by CVD techniques. In this case, the difference in thermal expansion is huge, and the high temperature deposition results in the production of high residual stresses in coating and substrate, which may significantly modify the system properties, especially adhesion. Theoretical modelling of the residual stress field may be useful for guiding the design process of a coating and the choice of materials suitable as substrates or possible buffer layers between metal and coating [1]. However, predictions are limited by the generally poor knowledge of the actual mechanical and thermal properties of the materials in use (e.g., Young's modulus (E) and thermal expansion coefficient (α) of CVD diamond differ considerably from values for bulk diamond [2,3]) and by the approximate modelling of the microstructure. The latter may be important in determining coating properties; for instance, diamond texture, which depends largely on the CVD conditions and substrate properties, has a great influence on coating roughness, which in turn influences the tribological properties.

X-ray diffraction methods offer a unique opportunity to measure the orientation distribution in the coating and the residual strain field in both coating and substrate and possible interfacial compounds. This is particularly important when we consider diamond deposition on Ti-based materials, for which a complex process involving diamond growth, carbon diffusion in the metal, and carbide formation at the interface [4–6] is expected to occur.

2. Experimental

The diamond films were grown in a CVD reactor [6] by using a 1% CH_4/H_2 activated by a Ta filament kept at 2180°C. The experimental conditions were as follows:

* Corresponding author.

PII S0925-9635(96)00605-X

pressure, 36 Torr; gas flow rate, 200 sccm; $T_{sub}=650°C$. The deposition runs lasted 30, 90, and 180 min, respectively. Substrates used were Ti–6Al–4V plates ($20\times10\times3\ mm^3$), polished with 6-μm diamond paste, scratched under controlled conditions with 25-μm diamond paste, and thoroughly cleaned ultrasonically in an acetone bath.

XRD measurements were conducted both by a conventional laboratory instrument (Huber 4030 Stress/texture) and by means of SR at Station 2.3 of the Daresbury facility (DRAL, Warrington, UK) [7]. In both cases, the diffraction geometry was based on a four-circle goniometer and a parallel beam with monochromator in the incident path; the overall reliability of the measurements was carefully checked by measuring a zero-stress powder sample [8].

The preliminary X-ray residual stress analysis (XRSA) and texture measurements performed by the laboratory instrument were done using Cu Kα radiation and a gas-filled position-sensitive detector (PSD). SR-XRD was conducted by using wavelengths appropriate for studying the three main phases present in the coated Ti-alloy: diamond, Ti, and TiC. For each phase studied, the wavelength for XRSA was selected so as to produce a detectable reflection (i.e., sufficiently intense and free from other overlapping peaks) in the high angle region of the pattern, where the sensitivity of the method is higher and errors are minimized.

XRSA was performed following the standard methods reported in the literature [9]; stress data were calculated from the slope of the "$\sin^2\psi$" plot, using the appropriate X-ray elastic constants (XECs) calculated from single-crystal stiffness data [9,10].

3. Results

The traditional "$\sin^2\psi$" analysis [9] performed on the data collected by the laboratory instrument showed a high compressive stress in the diamond layer. As shown in Fig. 1, the same type of measurement repeated after 7 months gave the same slope in the "$\sin^2\psi$" plot, demonstrating the stability of the residual stress field in the coated component. Moreover, there was no data splitting for positive and negative ψ-tilting or different ϕ-rotations (in-plane angle) [8]. These results suggest the presence of a simple axially symmetric residual stress field in the coating, with

$$\sigma_{11}=\sigma_{22},\ \sigma_{33}=0,\ \sigma_{ij}=0\ (i\neq j), \quad (1)$$

where σ_{11} and σ_{22} are the in-plane components and σ_{33} is perpendicular to the surface. This result agrees with previous findings on CVD diamond deposited on WC–Co substrates [8], and seems to be a peculiarity of CVD diamond.

The (220) and (111) diamond pole figures (Fig. 2) show that diamond had a [hh0] fiber texture, irrespective of the deposition time (and therefore thickness). However, the preferred orientation was more marked for the thicker sample, and in any case a considerable mosaicity was present, as indicated by the large width of the (220) pole. The other phases showed no preferred orientation, as demonstrated by the lack of features in the (220) pole figure of TiC in Fig. 3.

Synchrotron radiation enabled us to perform the XRSA in the three main phases, using the wavelengths reported in Table 1. Due to carbon diffusion, the Ti–6Al–4V matrix was referred to as α-Ti(C). Table 1 also reports XECs values, Miller indices of the studied reflections, and the information depth, defined as ($\xi_i=\sin\theta\cos\phi/2\mu$). E and υ are the Young modulus and the Poisson ratio, respectively.

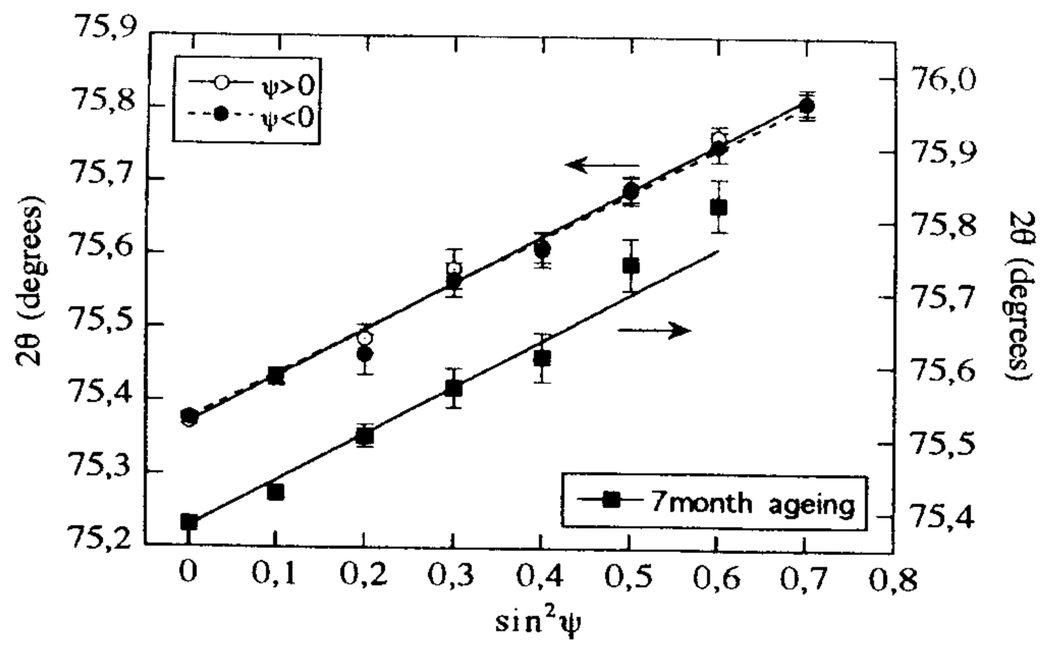

Fig. 1. "$\sin^2\psi$ plot" for the (331) diamond peak of the sample deposited for 180 min. Positive and negative ψ-tilting (left) and same analysis (positive tilting only) after a 7-month ageing.

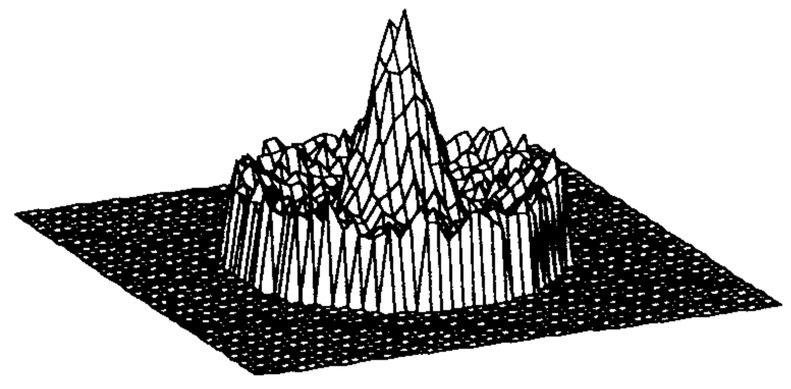

(b)

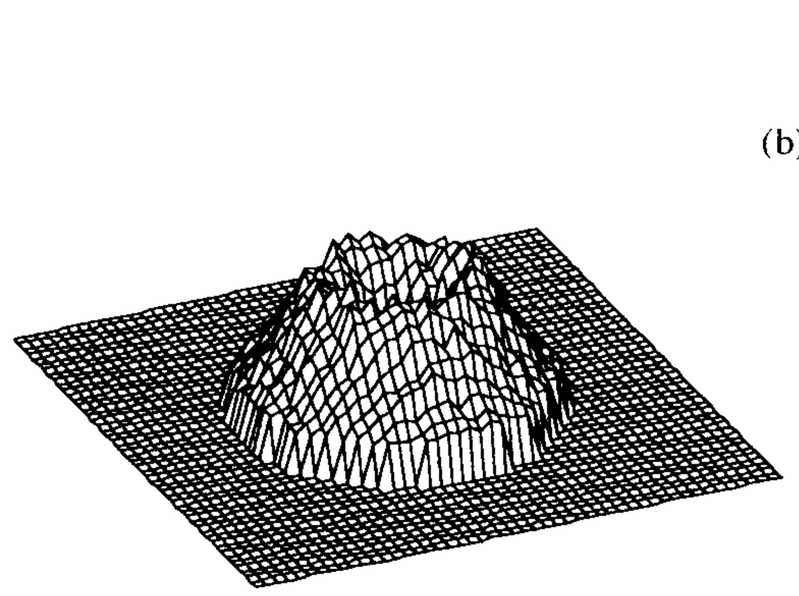

Fig. 2. (220) (a) and (111) (b) diamond pole figures for the sample of Fig. 1.

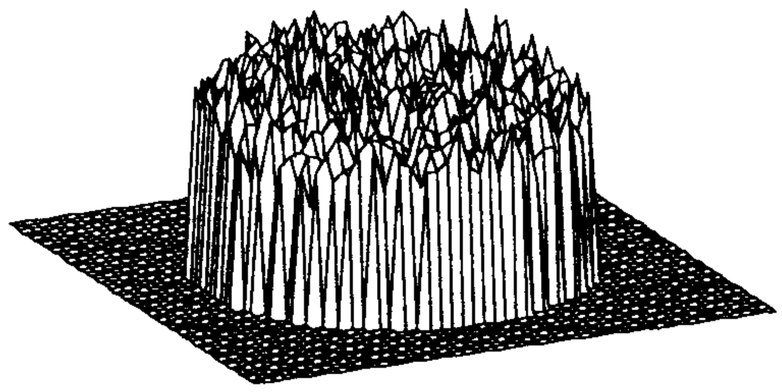

Fig. 3. (220) TiC pole figure for the sample of Fig. 1.

Table 1
Wavelengths, XECs, and Miller indices of measured reflections

	Phase			
	Diamond	TiC	α-Ti(C)	
Wavelength (Å)	2.15	1.66	1.68	1.4
(hkl)	(220)	(024)	(121)	(025)
$XEC_1=(1+\upsilon)/E$	9.2×10^{-4}	2.73×10^{-3}	1.13×10^{-2}	
$XEC_2=-\upsilon/E$	-5.5×10^{-5}	-4.50×10^{-4}	-2.7×10^{-3}	
ξ_i (at $\psi=45°$) (μm)	72.2	4.8	2.8	8.6

The "$\sin^2\psi$" plots for the three phases in the sample deposited for 180 min are reported in Fig. 4. The strain-free interplanar distances were experimentally measured at ψ-tilting angles calculated from the following relation, which is verified for a biaxial stress field [9]:

$$\sin^2\psi\,(\epsilon=0)=\frac{2\upsilon}{1+\upsilon}+\frac{XEC_2}{XEC_1} \quad (2)$$

The different slopes in Fig. 4 clearly demonstrate the trend of the stress field inside the coated component, that is, highly compressive in diamond and TiC and tensile in the metal matrix. The residual stress in the α-Ti(C) must be considered as an effective value, because of the simultaneous presence of a compositional gradient due to carbon diffusion, along with the residual strain (probably a gradient of strain as well). Under such conditions, the two effects can hardly be separated [11]. However, to have an idea of the trend inside α-Ti(C), the XRSA in the metal was repeated by using a shorter wavelength: results were comparable (97(10) MPa), indicating no sharp changes in the stress/compositional field within the information depth (see Table 1). The stress values obtained from the data in Fig. 4, using the simple model of Eq. (1), are schematically reported in Fig. 5, which also shows the phase stacking sequence. Such detailed information on the stress field in a coated component could hardly be obtained by means of other analytical techniques. The same analysis carried out on the Ti–6Al–4V alloy, coated by the thinner (30 min) diamond film, gave a very similar result: a highly compressive stress in diamond (−6.2(3) GPa) and TiC (−1.51(7) GPa), and a tensile (effective) stress in α-Ti(C) (42(6) MPa).

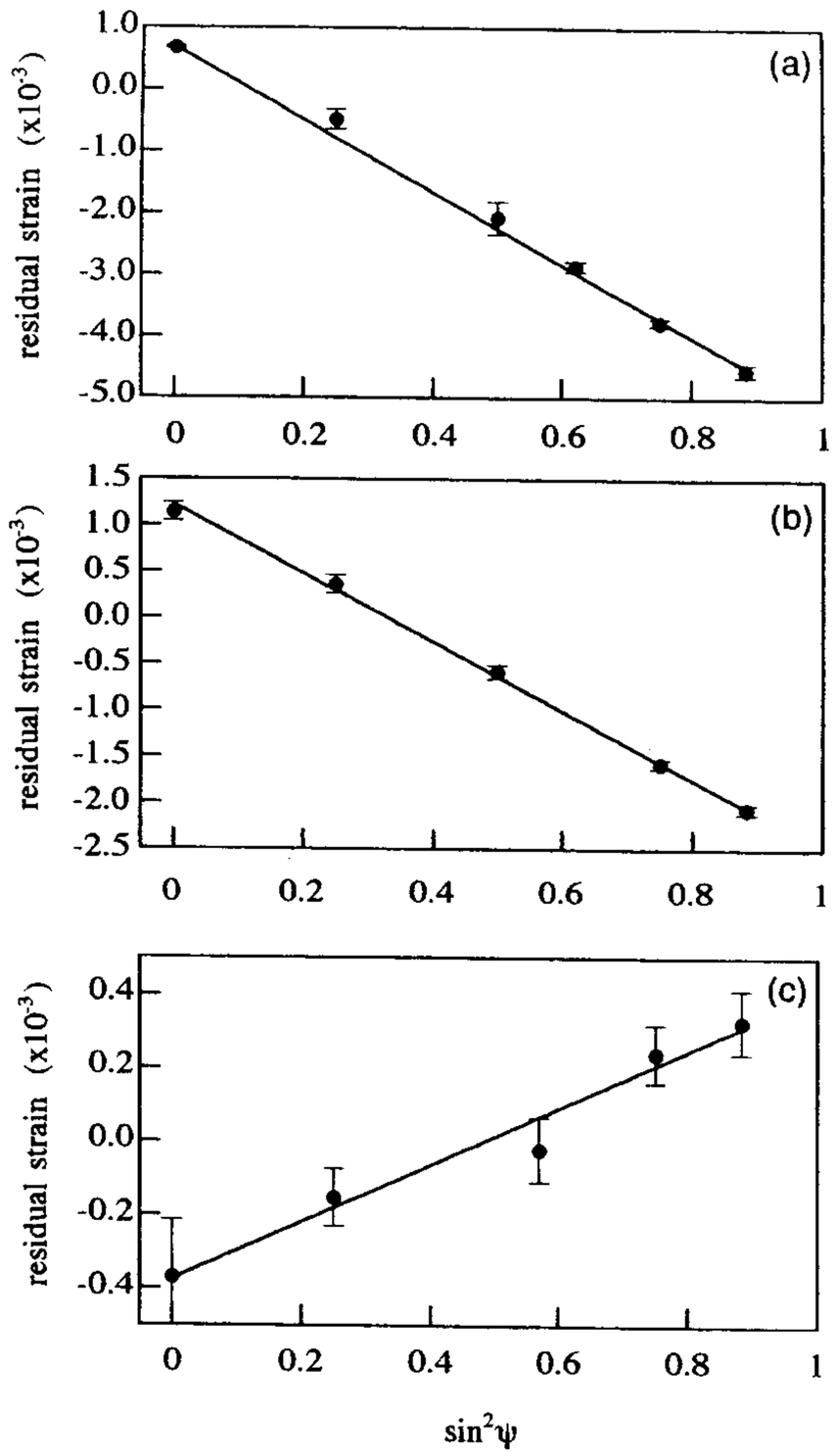

Fig. 4. "Sin² ψ plot" from synchrotron radiation XRSA for the sample of Fig. 1; (a) diamond (331), (b) TiC (024) and (c) α-Ti(C) (121).

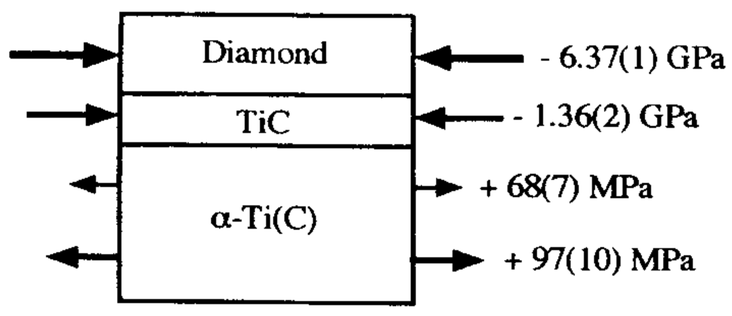

Fig. 5. Schematic representation of the residual stress field calculated from the data of Fig. 4 and the model expressed by Eq. (1).

Finally, it is interesting to study the effect of such a high residual strain in the diamond layer on the experimental determination of texture by the pole figure method. When a high residual strain is present, the peak maximum in the pole figure is shifted as a function of the ψ-(α) tilting angle, and a fixed 2θ position does not correspond any longer to the maximum. Under such conditions, a measure of the integrated intensity would be more meaningful. Given the symmetry of the pole figure (fiber texture, Fig. 2), this type of information is already available from the experimental data for the "$\sin^2\psi$" analysis. Fig. 6 shows the comparison of a fixed-ϕ(β) measurement of peak maximum (at fixed 2θ)

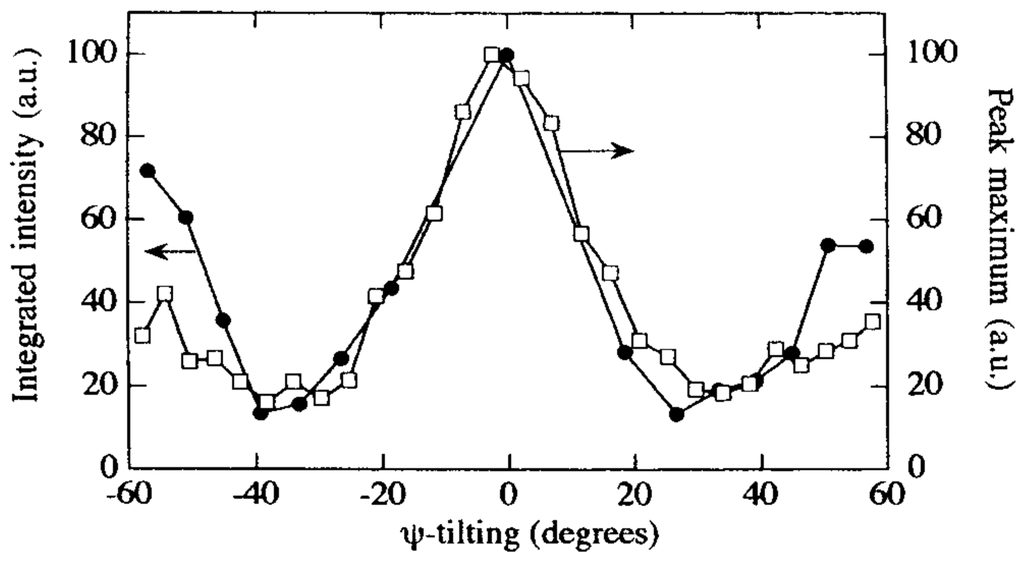

Fig. 6. Effect of the residual strain on texture analysis: fixed-β measurement of the peak maximum (right) and integrated intensity (left) for the sample 180 min at 650°C.

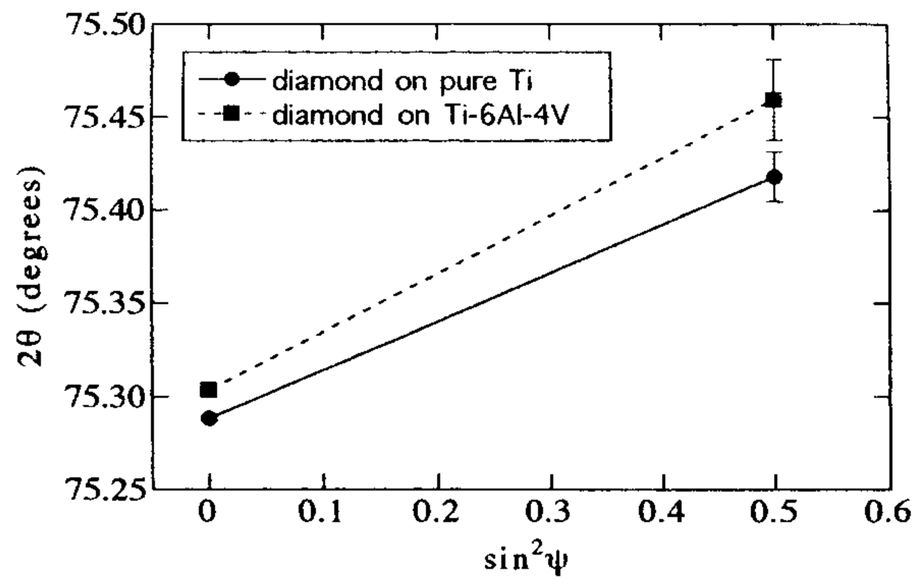

Fig. 7. XRSA for two samples of pure Ti and Ti–6Al–4V, respectively. Same polishing (1-μm diamond paste) and deposition conditions (180 min at 650°C, 1% CH_4). Due to the high preferred orientation, the double tilt method was employed [9].

and the corresponding integrated intensity, obtained by profile modelling of the PSD signal [12]. The two patterns are qualitatively the same, but differ considerably in the high tilting angle region, where the effect of the residual strain is more pronounced.

4. Discussion and conclusions

Several comments may be made on the present results. The measured residual stress in the diamond layer is very high, and probably slightly above the thermal stress, σ_T. In fact, σ_T, calculated as $\Delta\alpha \cdot \Delta T \cdot E\upsilon/(1-\upsilon)$ is of the order of -6 GPa, even though a correct calculation of the thermal stress needs a direct knowledge of thermal expansion coefficients and elastic moduli of the present materials, as a function of the temperature. If the thermal stress contribution is of the order of 6 GPa, the presence of some mechanism of compressive intrinsic stress generation must be invoked. Film porosity and presence of impurity, are thought to produce such additional compressive stress. According to Windischmann et al. [13] compressive intrinsic stress, detected in polycrystalline diamond coatings, could be ascribed to the co-deposition at grain boundaries of non-diamond carbon phases.

As a second remark, the measured residual stress was much higher than that previously found in a diamond layer produced under the same conditions on pure Ti. In this case [5], the residual stress was -2.8 GPa in diamond and was tensile in both TiC and α-Ti(C) (390 and 110 MPa, respectively). Possible explanations for this discrepancy include the much lower yield stress of pure Ti as compared with the Ti–6Al–4V alloy, and the presence of different minority phases at the metal/ceramic interfaces. In fact, the lower mechanical resistance of pure Ti could allow a partial relaxation of the high thermal stress. With regard to the different compositions of the interfacial layers, TiH_2 and TiC were found in the case of pure Ti [4–6], whereas mixed Al,V carbide phases were found in the XRD pattern of the coated Ti–6Al–4V.

A third possible interpretation could be connected with surface roughness. The roughness of the present samples (Ti–6Al–4V), completely different from that of pure Ti substrates [5], could be responsible for the different growth kinetics of the various phases at the metal/ceramic interface and hence the different mechanical adhesion of diamond.

Preliminary measurements in two samples, pure Ti and Ti–6Al–4V with same size and surface finishing, showed the presence of compressive residual stresses of $-3.8(5)$ and $-3.1(3)$ GPa, respectively, which values are comparable within the experimental errors (Fig. 7. In this case, surface roughness seems to be the key parameter controlling the residual stress field. This hypothesis is supported by recent studies on the diamond/Ti system [14]. The measurements in this case pointed out compositional inhomogeneous interfacial layers (graphite, TiH_2, TiC) related to local surface topography, with graphite mainly accumulated on the relief size of the scratched surface, and TiC and TiH_2 formed in the hollows between the protruding edges. Surface morphology was therefore found to affect the formation of the various phases at specific locations of the substrate, and this suggests that the surface roughness could determine texture and residual stress of the diamond coatings.

Considering the promising protective and anti-wear functions expected for diamond-coated Ti-alloy, further SR-XRD investigations of differently polished samples are planned, to improve our knowledge of such complex systems and to control the experimental procedures that can help in relieving residual stress and enhancing film adhesion.

References

[1] J.K. Wright, R.L. Williamson and K.J. Maggs, *Mater. Sci. Eng., A 187* (1994) 87–96.

[2] H. Windischmann and K.J. Gray, *Diamond Relat. Mater., 4* (1995) 837–842.
[3] D.J. Pickrell, K.A. Kline and R.E. Taylor, *Appl. Phys. Lett., 64(18)* (1994) 2353.
[4] G. Cappuccio, M. Leoni, P. Scardi, V. Sessa and L. Terranova, *Mater. Sci. Forum, 203* (1996) 285–290.
[5] P. Scardi, M. Leoni, V. Sessa, M.L. Terranova and G. Cappuccio, *Mater. Sci. Forum, 228–231* (1996) 451–456.
[6] M.L. Terranova, V. Sessa, M. Rossi, G. Vitali, G. Cappuccio and C. Veroli, *J. Phys. IV, C5* (1995) 879–886.
[7] R.J. Cernik, P.K. Murray, P. Pattison and A.N. Fitch, *J. Appl. Cryst., 23* (1990) 292–296.
[8] P. Scardi, M. Leoni and S. Veneri, to be presented at the 45th Annual Denver X-Ray Conference, Denver 8/96. Submitted for publication in *Adv. X-Ray Analysis*, 40.
[9] I.C. Noyan and J.B. Cohen, *Residual Stress Measurement by Diffraction and Interpretation*, Springer-Verlag, New York, 1987.
[10] J. Wilks and E. Wilks, *Properties and Applications of Diamond*, Butterworth-Heinemann, Oxford (UK), 1991.
[11] R. Delhez, Th.H. de Keijser and E.J. Mittemeijer, *Surf. Eng., 3* (1987) 331.
[12] P. Scardi and M. Leoni (1996) Unpublished results.
[13] H. Windischmann, G.F. Epps, Y. Cong and R.W. Collins, *J. Appl. Phys., 69* (1991) 2231.
[14] M.L. Terranova, M. Rossi and G. Vitali, *J. Appl. Phys., 80* (6) (1996) 3552.